THE JOURNAL OF PHYSICAL CHEMISTRY A

Article

pubs.acs.org/JPCA

Spectroscopy of the C−H Stretching Vibrational Band in Selected Organic Molecules

Jiří Šebek,[†,§] Roie Knaanie,[†,§] Brian Albee,[‡] Eric O. Potma,[‡] and R. Benny Gerber*[,†,‡]

[†]Institute of Chemistry and The Fritz Haber Research Center, The Hebrew University, Jerusalem 91904, Israel

[‡]Department of Chemistry, University of California, Irvine, California 92697, United States

ABSTRACT: The vibrational spectroscopy of C−H stretches in organic molecules is of considerable importance for the characterization of these systems and for exploration of their properties. These stretches are strongly anharmonic, and thus methods including anharmonicity have to be used. The vibrational self-consistent field (VSCF) is applied to the following organic compounds: acetone, dimethylacetylene, neopentane, toluene, ethylene, and cyclopropane. The computed spectra are compared to new experimental data, including Raman measurements of all molecules except cyclopropane and IR of acetone, neopentane, and ethylene. A high level of agreement is found for all of the molecules. The characteristic features of CH_3 and CH_2 groups are studied and analyzed in detail. A reliable, unambiguous assignment of vibrational modes to spectral peaks is provided. Several characteristic features of CH_3 and CH_2 vibrations in polyatomic molecules are clarified, providing easier assignments for different types of organic molecules.

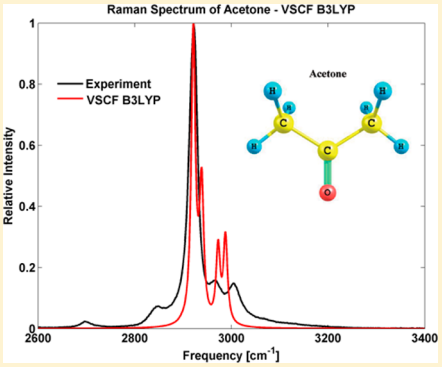

1. INTRODUCTION

Hydrocarbons as gases or liquids are a primary energy source and are of great importance in several disciplines of chemistry including petroleum chemistry,[1,2] environmental chemistry,[3] and geological and planetary chemistry.[4,5] The nature of a hydrocarbon or the hydrocarbon part of bio-organic molecule can be identified by observing the carbon−hydrogen stretching vibrational band in the region between 2800 and 3100 cm^{-1}. The C−H stretching vibrational band is usually isolated in the vibrational spectrum and has a high spectral intensity; therefore, this band is ideal for detection of the hydrocarbon part of biological molecules. Depending on the symmetry of the molecule, its vibrational modes may give rise to IR absorption or Raman scattering or both. The observed IR and Raman frequencies are the same, but their intensities are different and give additional spectral information. Nonlinear Raman microscopy techniques,[6−8] which enable real-time imaging of cells and tissue materials, use the strong C−H stretching band signature for mapping of carbohydrates, lipids, sterols, and proteins.[9] C−H stretching bands are also used for probing aliphatic molecules at surfaces.[10,11]

Despite the importance of the C−H stretching in vibrational spectroscopy of bio-organic molecules, assigning the vibrational modes that constitute the C−H stretching band profile remains a challenge. The CH-stretching vibrational range is characterized by several overlapping fundamental modes, overtone modes, and various combination modes, resulting in complicated band profiles that are poorly understood. This study aims to provide a better understanding of the C−H stretching band profile, by computational examining the vibrational spectrum of six simple organic compounds: acetone, dimethylacetylene, neopentane and toluene, which all contain the CH_3 group, and ethylene and cyclopropane, which contain the CH_2 group. The computed spectra are compared to the experimental IR and Raman data. The assignments of the vibrational modes of CH_3 and CH_2 groups are studied and analyzed in detail. Good agreement of the calculated anharmonic frequencies with the experimental ones is found.

Experimental and computational studies of the vibrational spectrum of hydrocarbons such as butane have been carried out by Murphy et al.[12] and by Durig et al.[13,14] In these studies both IR and Raman spectra of *n*-butane and many of its derivatives were computed at the harmonic level, using empirical scaling factors to correct the effects of anharmonicity. For the lower-frequency region of the spectra good agreement with experiment was found in these studies. However, rather large deviations were found for the high-frequency region. Harmonic calculations are computationally feasible even for very large organic molecules, but the accuracy of the harmonic approximation is insufficient,[15−17] in particular for stretching vibrations. C−H stretches of hydrocarbons show large anharmonic shifts with up to 10% deviation from the harmonic result;[18,19] therefore, anharmonic vibrational methods are desirable.

Anharmonic calculations for large molecules are challenging. The main difficulty is that anharmonic polyatomic Hamiltonians are inherently nonseparable. Several methods have been

Special Issue: Joel M. Bowman Festschrift

Received: February 9, 2013
Revised: June 16, 2013
Published: June 17, 2013

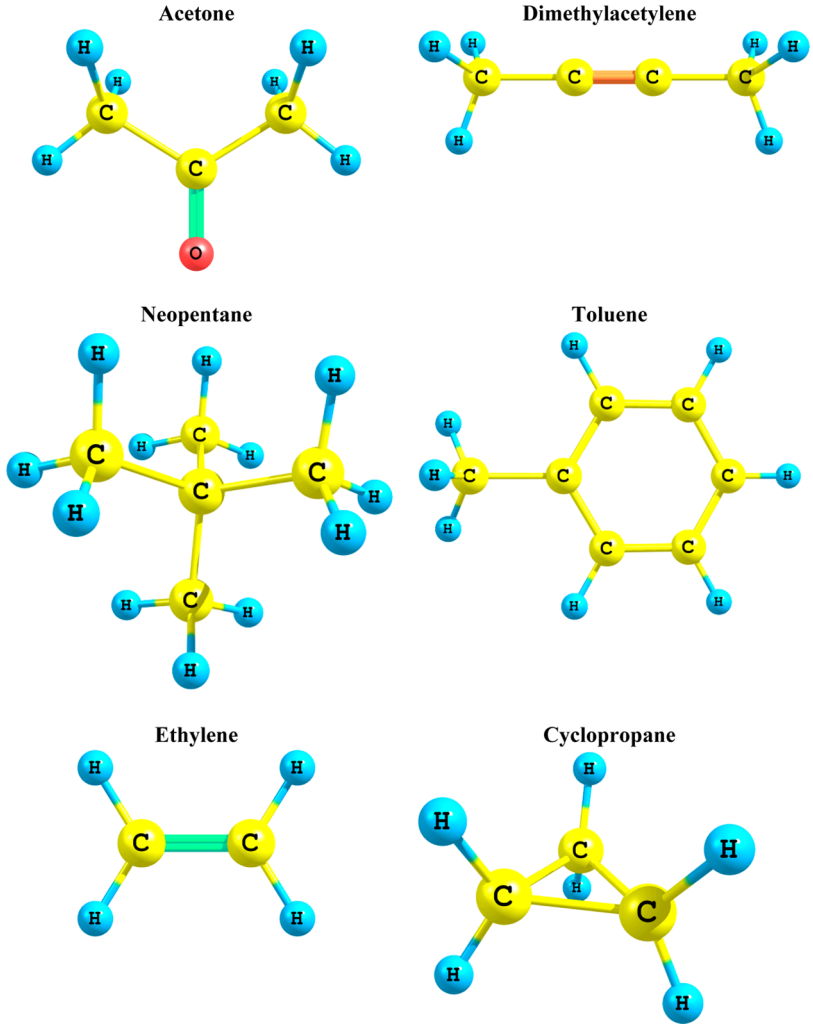

Figure 1. Geometrical structure of acetone, dimethylacetylene, neopentane, toluene, ethylene, and cyclopropane molecules.

proposed for computing anharmonic spectra of large systems. For exapmle, Gregoire et al.[20] and Gaigeot and Sprik[21] have applied the Car−Parrinello[22] molecular dynamics simulation on biological molecules. Barone implemented an efficient algorithm based on perturbation correction for the harmonic approximation.[23] This method is included in the GAUSSIAN[24] program package.

In this study we calculate anharmonic stretching vibrations of hydrocarbons by applying the VSCF (vibrational self-consistent field) approximation,[15,25−27] using a variant that directly employs ab initio potential surfaces. This direct ab initio method does not demand fitting of potential energy surfaces, nor applying empirical parameters or scaling factors[28,29] and is calculated from first principles. The VSCF algorithm is a part of the GAMESS[30] electronic structure package, and has been extensively and successfully applied in recent studies on many systems with up to 20−30 atoms.[18,31,32] A short description of the VSCF method can be found in the Methodology section. The accuracy of the VSCF approach depends on the basis set and the applied electronic structure method, such as BLYP, B3LYP,[33,34] and MP2,[35] which are used by the quantum chemical programs. In this research we made a comparison of the performances of these potentials. We have found that B3LYP potential performs very well for all cases and seems superior to MP2 for these systems.

On the basis of the good agreement of the calculations with the experimental results, we provide an assignment for the peaks of the spectral C−H band for all the molecules, which appear reliable and robust.

This paper is organized as follows: The IR and Raman measurements, and the anharmonic VSCF and VSCF-PT2 calculation methods are described in section 2. Results and discussion of the VSCF calculations with comparison to the experimental IR and Raman data are presented in section 3 and conclusions are given in section 4.

2. METHODOLOGY

a. IR Measurements. The IR measurements in this study were carried out using a Nicolet Magna-IR 860. All spectra were collected with a resolution of 0.964 cm^{-1}. A total of 100 measurements were averaged to improve signal-to-ratio. A CaF_2 sealed cell (Perkin-Elmer) with a path length of 0.025 mm was used to collect spectra on liquid hydrocarbon samples. Gas phase samples (ethylene and neopentane) were measured using a gas cell (Pike Technologies) with a path length of 100 mm and 4 mm thick KBr windows with a 25 mm diameter.

b. Raman Measurements. The Raman measurements in this study were performed on a home-built Raman system. A 532 nm diode pumped continuous wave laser (CrystaLaser) was used as the excitation source. The experimental layouts for

dx.doi.org/10.1021/jp4014674 | J. Phys. Chem. A 2013, 117, 7442−7452

the liquid and gas phase measurements were different. Raman spectra of liquid hydrocarbon samples were acquired using an inverted microscope system (Olympus IX71) equipped with a 20X, 0.75NA objective lens. The excitation beam was focused by the objective into the sample and the Raman scattered light was collected in the epi-direction. A holographic notch filter (Kaiser) was used to separate the Raman scattered light from the excitation light. The Raman scattered light was guided to a spectrometer (Andor Shamrock) outfitted with a CCD camera (Andor iDus). A custom cuvette was constructed with a 0.170 mm glass bottom, which was placed on the microscope stage to collect spectra. For these measurements, an integration time of 0.5 s was used, and up to 200 spectra were averaged to improve signal-to-noise.

Raman spectra for gas samples were obtained using a custom-built aluminum cell with glass windows and a folded path length of 50 cm. Pressures of up to 2 atm were used in the measurements. The excitation beam was sent through the cell, filtered at the output of the cell with a band-edge filter (Semrock), and directed to the spectrometer for detection. For these measurements, an integration time of 3 s and 300 accumulations were used to obtain good quality spectra.

c. Geometry Optimizations and Harmonic ab Initio Calculations. Geometry optimizations, and harmonic vibrational calculations were performed for all molecules by the DFT methods, BLYP and B3LYP,[33,34] and by the second-order Møller−Plesset perturbation theory (MP2) method.[35] Calculations were performed using the electronic structure program GAMESS.[30] Figure 1 shows the calculated geometrical structure of acetone, dimethylacetylene, neopentane, toluene, ethylene, and cyclopropane molecules. We used the correlation consistent polarized valence double-ζ basis set (cc-pVDZ) proposed by Dunning[36,37] in all calculations. The cc-pVDZ basis is feasible for VSCF calculations for systems with 10−20 atoms, and its accuracy is acceptable for comparison with experiment as previous studies have shown.[18,19,38] Anharmonic ab initio Vibrational Self-Consistent Field (VSCF) calculations were carried out by GAMESS, for an isolated molecule at T = 295 K. The following paragraphs describe the VSCF and VSCF-PT2 computational methods that were used in this research.

d. Vibrational Self-Consistent Field (VSCF) Methods. Anharmonic interactions including coupling between different modes were treated in this study within the VSCF method and its extensions.[15,17,25,27,39−50] Detailed systematic description of the method can be found also in a recent review by Roy and Gerber.[51] The origin of this approach is published in the work from the late 1970s by Bowman[25] and Gerber and Ratner.[39] The VSCF method is based on the approximation of separability; i.e., for a system with N vibrational degrees of freedom, the total vibrational wave function is represented by a product of one-dimensional wave functions

$$\Psi_n(Q_1,...,Q_N) = \prod_{j=1}^{N} \Psi_j^{(n)}(Q_j) \tag{1}$$

(Q_j are mass-weighted normal coordinates). The VSCF approximation reduces the problem of solving the N-dimensional vibrational Schrödinger equation to solving N single-mode VSCF equations. For each single-mode wave function, a mean field potential that includes the average effects of the other modes is employed. The potential of the system

$$V(Q_1,...,Q_N) = \sum_{j=1}^{N} V_j^{\mathrm{diag}}(Q_j) + \sum_i \sum_{j>i} V_{ij}^{\mathrm{coup}}(Q_i,Q_j) \tag{2}$$

is represented by the sum of separable single mode $V_i^{\mathrm{diag}}(Q_i) = V(0,...,Q_i,...,0)$ and pair-coupling terms $V_{ij}^{\mathrm{coup}}(Q_i,Q_j) = V(0,...,Q_i,...,Q_j,...,0) - V_i^{\mathrm{diag}}(Q_i) - V_j^{\mathrm{diag}}(Q_j)$, neglecting triplets and higher-order coupling interactions. The diagonal (single-mode) and coupling terms of the potential are calculated directly from the electronic structure program on 16 point grids along each normal coordinate, and on 16 × 16 square grids for each pair of normal coordinates. The calculated potentials are then used for numerical solution of the one-dimensional VSCF equations. A self-consistent field approach is used; i.e., all the equations are solved numerically until convergence is reached. The VSCF method and its extensions are discussed in detail in many previous publications.[15,26,27,40,52]

e. VSCF-PT2. The VSCF results can be improved using second-order perturbation theory (VSCF-PT2), also referred to as CC-VSCF.[53,54] This method is analogous to the Møller−Plesset method known in the context of electronic structure.[35] The PT2 correction is described by the following equation:

$$E_n^{\mathrm{PT2}} = E_n^{(0)} + \sum_{m\neq n} \frac{|\langle \prod_{j=1}^{N} \Psi_j^{(n)}(Q_j)|\Delta V| \prod_{j=1}^{N} \Psi_j^{(m)}(Q_j)\rangle|^2}{E_n^{(0)} - E_m^{(0)}} \tag{3}$$

where $\Psi_j^{(n)}(Q_j)$ is the anharmonic vibrational wave function corresponding to the normal modes Q_j of the state (n). ΔV is the difference between the correct Hamiltonian and the VSCF Hamiltonian; therefore, the correlation effects are all included in ΔV. E_n^{PT2} is the VSCF-PT2 energy of state n, and $E_n^{(0)}$ is the VSCF energy for the same state. The summation is over all the other states. A detailed description of this method and its applications can be found in refs 55 and 56. Christiansen explored the contribution of adding higher orders of the perturbation theory to the VSCF method.[57] He found that the second-order treatment is optimal.

f. Modeling of IR and Raman Line Shapes. The spectral curves were constructed by our software, while the transitions were assumed to be Lorentzian bands with the full widths at the half-height (fwhh) of 10 cm^{-1} (this value was estimated according to the profile of the experimental spectrum). A similar approach was used for other systems, e.g., for some saccharides[32] and hydrocarbons.[18] For the IR calculated spectra, no thermal correction was used; both frequencies and intensities were obtained anharmonically. Anharmonic IR intensity was calculated by numerical integration over the transition dipole moment, and the initial and final VSCF states, using the GAMESS software. The backscattering nonresonance Raman intensities were calculated by a standard formula implemented in GAMESS. For the Raman calculated spectra, the temperature was set to 295 K and the intensity expression used is harmonically derived, the only anharmonic part of the Raman calculation are thus the frequencies. Both the experimental and calculated spectra were normalized selectively to the highest peak.

3. RESULTS AND DISCUSSION

a. Comparison of Spectra from B3LYP and MP2 Potential Surfaces. The IR VSCF spectra of acetone,

dx.doi.org/10.1021/jp4014674 | J. Phys. Chem. A 2013, 117, 7442−7452

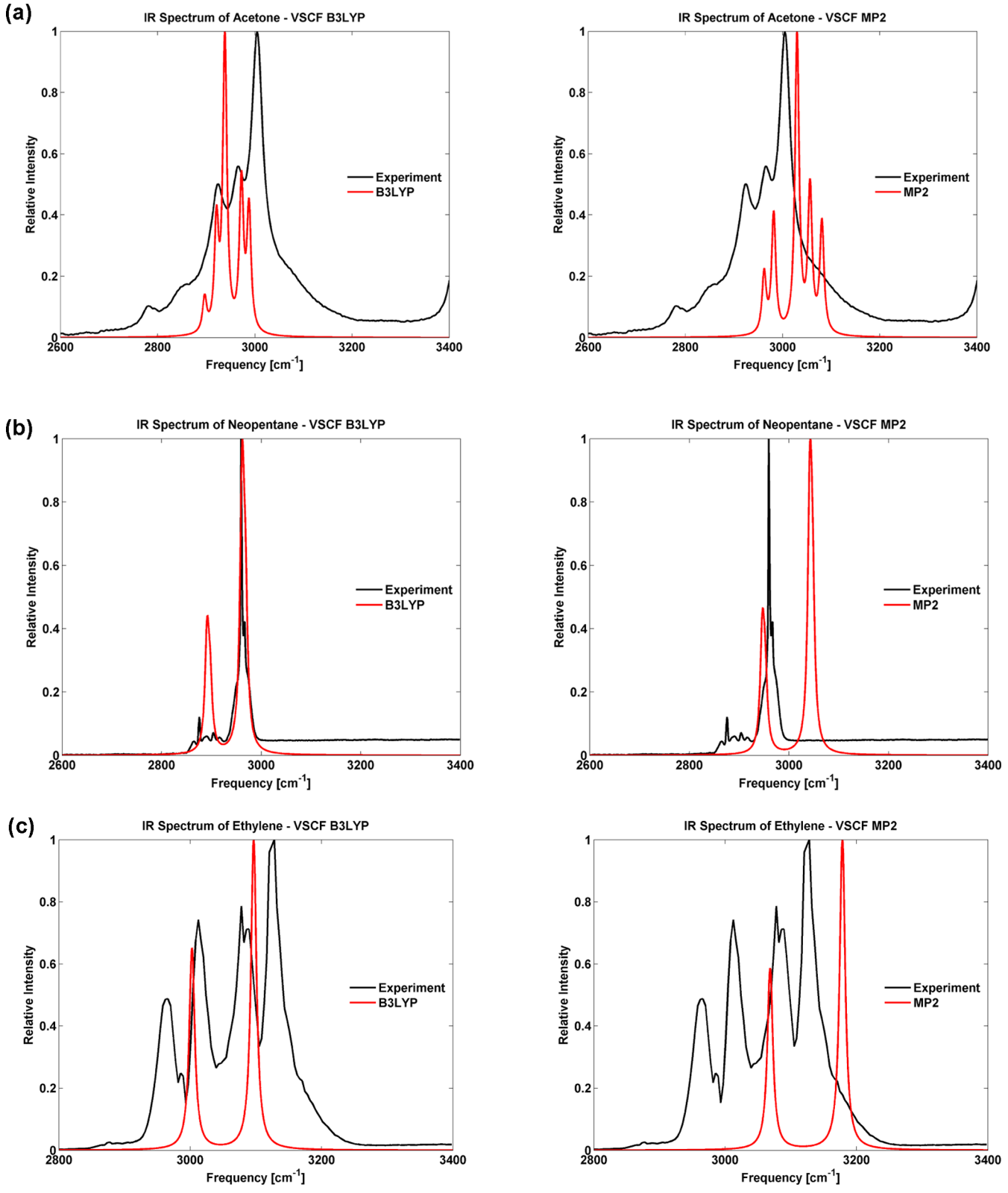

Figure 2. IR spectra of our set of organic molecules at the B3LYP (left) and MP2 (right) level (red line) compared to the experiment (black line): (a) acetone; (b) neopentane; (c) ethylene.

neopentane and ethylene and Raman VSCF spectra of acetone, dimethylacetylene, neopentane, toluene, ethylene, and cyclopropane calculated by B3LYP and MP2 methods are shown in Figures 2 and 3, including the comparison with experiment. Correspondingly, the computed vibrational frequencies and intensities for the stretching normal modes of acetone, dimethylacetylene, neopentane, ethylene, and cyclopropane at both the harmonic and the anharmonic level are shown in Tables 1−5. The tables show also a detailed comparison of the computational and the experimental Raman frequencies and

dx.doi.org/10.1021/jp4014674 | J. Phys. Chem. A 2013, 117, 7442−7452

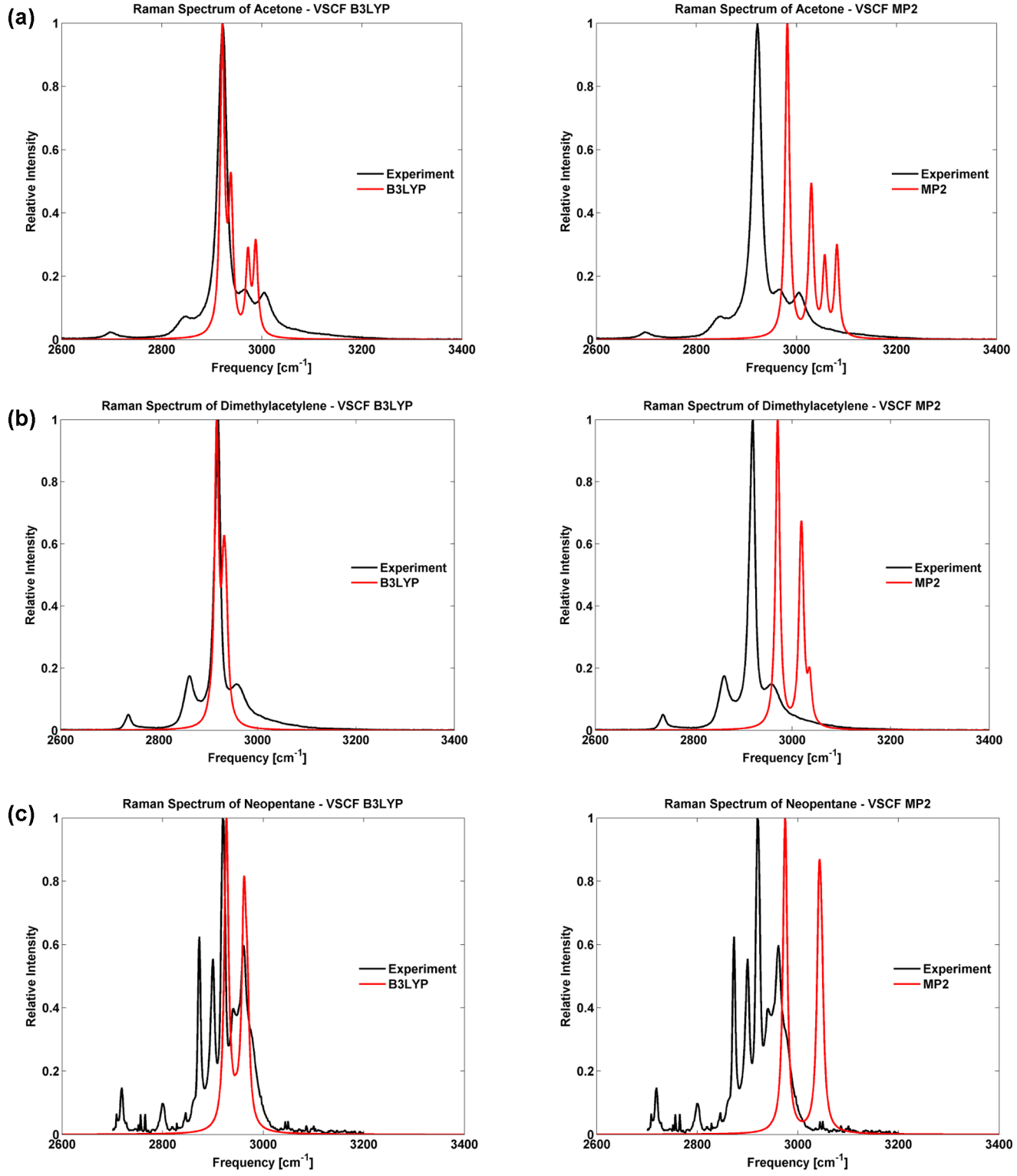

Figure 3. continued

dx.doi.org/10.1021/jp4014674 | J. Phys. Chem. A 2013, 117, 7442−7452

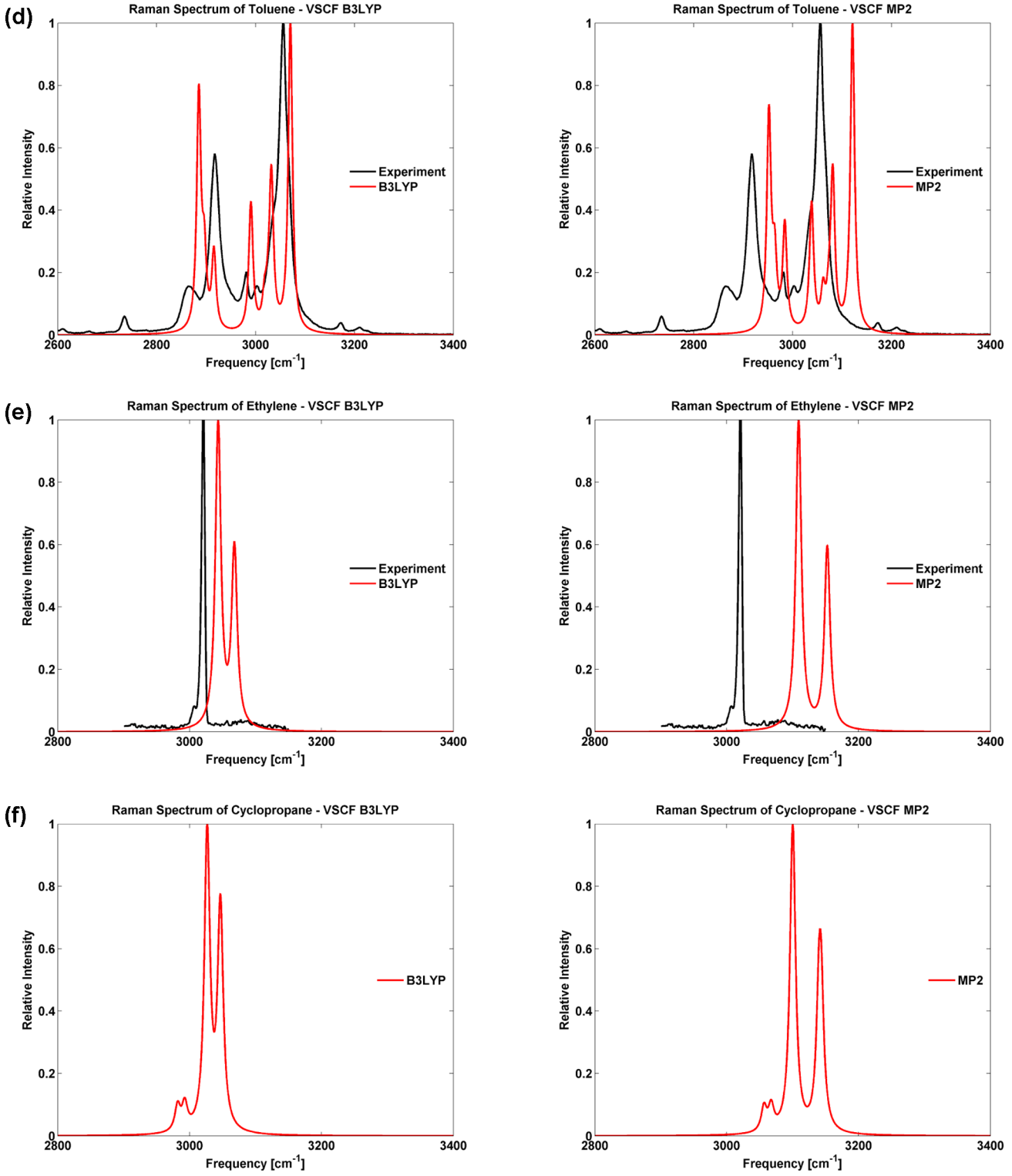

Figure 3. Raman spectra of our set of organic molecules at the B3LYP (left) and MP2 (right) level (red line) compared to the experiment (black line): (a) acetone; (b) dimethylacetylene; (c) neopentane; (d) toluene; (e) ethylene; (f) cyclopropane. In the case of cyclopropane, Raman measurements were not carried out in this work due to technical difficulties.

relative intensities (except for cyclopropane). In all cases we used the correlation consistent polarized valence double-ζ basis set (cc-pVDZ) proposed by Dunning.[36,37]

From the figures we can see that in all cases the frequencies are always the highest for MP2 and the lowest for BLYP. The comparison with experimental data shows very clearly that the calculated BLYP frequencies are always too small, as demonstrated in Figure 4. This method is thus not sufficient for VSCF spectra. Moreover, VSCF-PT2 frequencies are always smaller than those of VSCF (data not shown), which makes this effect even more apparent. However, the harmonic BLYP frequencies may seem the best. The reason is that the inaccuracy of the harmonic approximation always causes the increase of calculated frequency, whereas the BLYP functional

dx.doi.org/10.1021/jp4014674 | J. Phys. Chem. A 2013, 117, 7442−7452

Table 1. Vibrational Frequencies (cm^{-1}) of the CH_3 Stretching Modes in Acetone at Both the Harmonic and the Anharmonic Levels (Comparison between Computational Methods and Raman Experiment)[a,b]

	MP2/cc-pVDZ			B3LYP/cc-pVDZ							
mode	harm.	VSCF	VSCF-PT2	harm.	VSCF	VSCF-PT2	exp freq	VSCF IR intensity (km/mol)	relative VSCF Raman intensity	relative exp Raman intensity	mode type
30	3221	3081	3038	3150	2988	2950	3005	7.88	0.31	0.15	CH_3 asym
29	3220	3057	3034	3149	2972	2948	2963	9.58	0.27	0.16	CH_3 asym
28	3180	3030	3012	3095	2938	2919	not resolved	18.93	0.46	not resolved	CH_3 asym
27	3175	3025	3010	3088	2932	2914	not resolved	0.02	0.03	not resolved	CH_3 asym
26	3088	2982	2957	3031	2921	2891	2922	6.86	1.00	1.00	CH_3 sym
25	3083	2962	2950	3024	2897	2878	2849	2.2	0.00	0.07	CH_3 sym

[a]For acetone, the average difference between experimental and VSCF/B3LYP frequencies is 19 cm^{-1} (0.64%). The maximum frequencies difference is 48 cm^{-1} (1.68%). The average difference between relative experimental and relative VSCF Raman intensities is 8.46%. [b]The experimental and calculated relative Raman intensities in Tables 1−4 were normalized selectively to the highest peak.

Table 2. Vibrational Frequencies (cm^{-1}) of the CH_3 Stretching Modes in Dimethylacetylene at Both the Harmonic and the Anharmonic Levels (Comparison between Computational Methods and Raman Experiment)[a]

	MP2/cc-pVDZ			B3LYP/cc-pVDZ						
mode	harm.	VSCF	VSCF-PT2	harm.	VSCF	VSCF-PT2	exp freq	relative VSCF Raman intensity	relative exp Raman intensity	mode type
30	3179	3017	3003	3085	2931	2903	not resolved	0.23	not resolved	CH_3 asym
29	3179	3020	3006	3085	2933	2909		0.22		CH_3 asym
28	3178	3020	3017	3084	2936	2897		0.13		CH_3 asym
27	3178	3036	2998	3084	2937	2911	2959	0.13	0.18	CH_3 asym
26	3085	2957	2947	3018	2917	2876	2922	1.00	1.00	CH_3 sym
25	3084	2971	2963	3018	2901	2885	not resolved	0.00	not resolved	CH_3 sym
24	2283	2248	2238	2371	2325	2275	2337	0.41	0.25	C≡C triple

[a]For dimethylacetylene, the average difference between experimental and VSCF/B3LYP frequencies is 13 cm^{-1} (0.47%). The maximum frequencies difference is 22 cm^{-1} (0.75%). The average difference between relative experimental and relative VSCF Raman intensities is 7.0%.

shows a clear tendency to decrease the frequencies. These two sources of systematic error are thus pointing into the opposite directions; therefore, the resulting frequencies seem to be good, as has been discussed previously.[38] The comparison of the electronic structure methods based on the harmonic calculation alone can thus lead to incorrect conclusions.

The competition between B3LYP and MP2 requires a more profound discussion. For most systems discussed in this article B3LYP seems superior to MP2. This fact is surprising because MP2 has been supposed to be more accurate than B3LYP;[38] however, it is in agreement with our results for butane.[19] In a recent study (in press),[58] it was found that a new hybrid MP2/MP4 potential yields very good agreement with experiment for acetone, better than both B3LYP and MP2 potentials. For almost all molecules here we can see a good agreement with experiment for B3LYP, whereas the MP2 frequencies appear too high. One exception to this trend is found in acetone, the MP2 IR spectrum of which is better than the B3LYP one; however, the acetone B3LYP Raman spectrum is superior to the MP2 results. The MP2 frequencies are slightly higher than the experimental maxima, whereas the B3LYP frequencies are slightly lower, the differences being similar. In this case, VSCF-PT2 spectra at the MP2 level seem the best. However, even for this molecule the spectra obtained by different methods are comparable and the PT2 correction does not convincingly improve the VSCF spectra. Therefore, for the rest of this article we have chosen the VSCF spectra at the B3LYP level, given the superiority of this method for most molecules described here. We can see in Figure 3 a very good agreement between B3LYP Raman spectra and experiment, even more than in the case of IR, for all molecules.

It should be noted that similar conclusions in this study are reached if the comparison is made using the VSCF-PT2 vibrational algorithm. For the systems studied here, there are cases of near degeneracy in the C−H band. In cases such as this, VSCF-PT2, which is not adapted for degeneracy is generally less reliable: in some degenerate cases VSCF-PT2 gives results better than VSCF; in other cases, the opposite is true. Moreover, we prefer to present results obtained by a simpler method, in cases where more advanced methods do not improve the results significantly. For these reasons we mostly presented in this work VSCF calculations. For comparison, we also gave VSCF-PT2 results. In Tables 1−5 we show the results for both the VCSF and VSCF-PT2 with the MP2 and B3LYP potentials for the tested compounds. We note here that for cases of quasi-degenerate bands such as the C−H band in butane, the accuracy of VSCF and VSCF-PT2 seems to be about the same.[18,19] Whichever method is used to calculate the vibrational spectra, the conclusions on the quality of the MP2 and B3LYP potentials are the same.

b. Comparison between VSCF B3LYP and Raman experiment. In Tables 1−4 the comparison between VSCF/B3LYP and Raman experiments show that the average differences between the experimental and VSCF/B3LYP

dx.doi.org/10.1021/jp4014674 | J. Phys. Chem. A 2013, 117, 7442−7452

Table 3. Vibrational Frequencies (cm^{-1}) of the CH_3 Stretching Modes in Neopentane at Both the Harmonic and the Anharmonic Levels (Comparison between Computational Methods and Raman Experiment)[a]

	MP2/cc-pVDZ			B3LYP/cc-pVDZ							
mode	harm.	VSCF	VSCF-PT2	harm.	VSCF	VSCF-PT2	exp freq	VSCF IR intensity (km/mol)	relative VSCF Raman intensity	relative exp Raman intensity	mode type
51	3165	3047	3034	3093	2962	2938	2961	86.68	0.35	0.60	CH_3 asym
50	3165	3042	3034	3092	2968	2936	not resolved	85.02	0.34	not resolved	CH_3 asym
49	3165	3043	3032	3091	2962	2944	not resolved	85.91	0.35	not resolved	CH_3 asym
48	3160	3046	3026	3086	2938	2919	2940	0.17	0.03	0.40	CH_3 asym
47	3160	3043	3028	3085	2945	2926	not resolved	0.62	0.01	not resolved	CH_3 asym
46	3159	3038	3029	3084	2953	2931		0.26	0.02		CH_3 asym
45	3159	3037	3028	3084	2946	2924		0.1	0.02		CH_3 asym
44	3159	3038	3029	3083	2955	2941		0.06	0.00		CH_3 asym
43	3068	2975	2944	3024	2927	2890	2919	0.03	1.00	1.00	CH_3 sym
42	3061	2946	2934	3013	2891	2875	2873	36.96	0.00	0.63	CH_3 sym
41	3061	2952	2948	3012	2892	2874	not observed	37.25	0.00	not observed	CH_3 sym
40	3061	2948	2937	3012	2897	2890	2900	37.54	0.00	0.55	CH_3 sym

[a]For neopentane, the average difference between the resolved experimental and VSCF/B3LYP frequencies is 6 cm^{-1} (0.22%). The maximum frequencies difference is 18 cm^{-1} (0.63%). The average difference between relative experimental and relative VSCF Raman intensities is 36.06%.

Table 4. Vibrational Frequencies (cm^{-1}) of the CH_2 Stretching Modes in Ethylene at Both the Harmonic and the Anharmonic Levels (Comparison between Computational Methods and Raman Experiment)[a]

	MP2/cc-pVDZ			B3LYP/cc-pVDZ							
mode	harm.	VSCF	VSCF-PT2	harm.	VSCF	VSCF-PT2	exp freq	VSCF IR intensity (km/mol)	relative VSCF Raman intensity	relative exp Raman intensity	mode type
18	3311	3179	3165	3233	3097	3083	not observed	23.6	0.00	not observed	CH_2 asym
17	3286	3153	3139	3205	3068	3053	3077	0	0.59	0.04	CH_2 asym
16	3206	3109	3055	3141	3043	2988	3021	0	1.00	1.00	CH_2 sym
15	3188	3069	3056	3124	3003	2990	3007	15.33	0.00	0.08	CH_2 sym

[a]For ethylene, the average difference between experimental and VSCF/B3LYP frequencies is 12 cm^{-1} (0.39%). The maximum frequencies difference is 22 cm^{-1} (0.72%). The average difference between relative experimental and relative VSCF Raman intensities is 21.23%.

Table 5. Vibrational Frequencies (cm^{-1}) of the CH_2 Stretching Modes in Cyclopropane at Both the Harmonic and the Anharmonic Levels

	MP2/cc-pVDZ			B3LYP/cc-pVDZ				
mode	harm.	VSCF	VSCF-PT2	harm.	VSCF	VSCF-PT2	VSCF Raman intensity	mode type
27	3304	3181	3162	3222	3094	3073	0.21	CH_2 asym
26	3286	3140	3124	3202	3047	3030	109.89	CH_2 asym
25	3286	3143	3124	3201	3046	3025	109.45	CH_2 asym
24	3198	3100	3064	3128	3027	2986	286.22	CH_2 sym
23	3187	3057	3042	3119	2982	2966	23.62	CH_2 sym
22	3187	3068	3042	3118	2993	2965	24.24	CH_2 sym

frequencies for acetone, dimethylacetylene, neopentane, and ethylene are 19, 13, 6, and 12 cm^{-1}, respectively (between 0.22% to 0.64%). The corresponding maximum frequencies differences are 48, 22, 18, and 22 (between 0.63% and 1.68%). This good agreement between B3LYP Raman spectra and experiment is presented also in Figure 3.

The average differences between the relative experimental and relative VSCF Raman intensities for acetone, dimethylacetylene, neopentane, and ethylene are 8.46%, 7.0%, 36.06%, and 21.23%, respectively. It is well-known that the errors on intensities are much larger than for frequencies. In this study the treatment of the widths of the lines, which is empirical and

dx.doi.org/10.1021/jp4014674 | J. Phys. Chem. A 2013, 117, 7442−7452

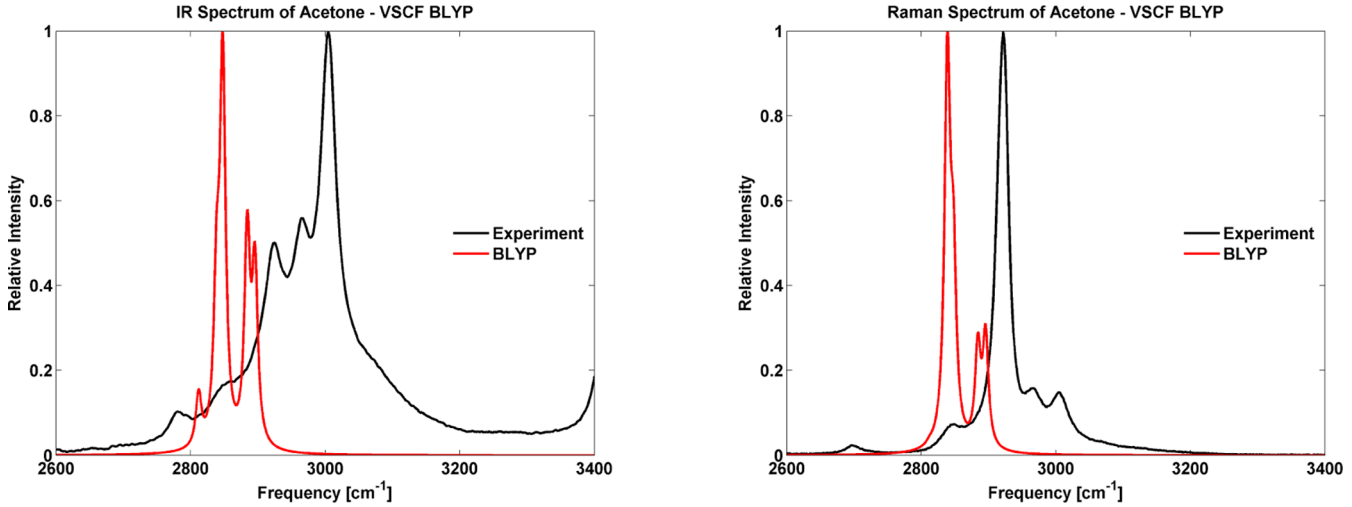

Figure 4. Calculated BLYP IR and Raman spectrum of acetone (red line) compared to the experiment (black line).

certainly not rigorous, may be one of the factors for the large differences for the intensities. The large discrepancy between the computed and experimental intensities, though certainly acceptable in the present state of the art, shows the importance of developing an improved treatment for vibrational spectroscopy lineshapes for systems at ambient temperatures.

c. The CH_3 Stretching Vibrations. In the spectra of all tested molecules containing CH_3 and not containing CH_2 groups, i.e., neopentane, acetone, dimethylacetylene, and toluene, two main absorption bands are present: the CH_3 symmetric and asymmetric stretches. These two bands are always clearly resolved. We can see this trend in both calculations and experiment. The toluene Raman spectrum contains one more band corresponding to aromatic C−H stretches; however, this band is clearly isolated from the other bands because of the higher frequencies of the corresponding modes. Therefore, it does not disturb in the analysis of CH_3 bands.

In Table 6, the calculated VSCF frequencies of both symmetric and asymmetric CH_3 modes of these molecules are shown. Butane modes which were published in ref 19 are added as a reference. The symmetric modes appear more or less at the same place for all molecules, around 2900 cm^{-1}. Only the toluene CH_3 symmetric mode frequency is somewhat lower (2885 cm^{-1}); however, this trend is not supported by the experimental data. For example, the toluene CH_3 symmetric experimental maximum is found at 2865 cm^{-1}, almost at the same place as the corresponding maximum of the other molecules studied here.

Table 6. Calculated Frequencies of C−H Vibrations in Molecules Containing CH_3 Groups

	CH_3 sym		CH_3 asym	
molecule	transitions	frequency range (cm^{-1})	transitions	frequency range (cm^{-1})
neopentane	4	2891−2927	8	2938−2968
acetone	2	2897−2921	4	2932−2988
dimethylacetylene	2	2901−2917	4	2931−2937
toluene	1	2885	2	2896−2916
butane[a]	2	2900−2920	2	2938−2954

[a]The results for butane were already presented in ref 19.

In Table 6 we can also see that both symmetric and asymmetric CH_3 vibrational frequencies of butane appear at the expected place. It supports our hypothesis that these CH_3 frequencies do not significantly depend on the surroundings of the functional group, and so the position of CH_3 absorption bands can always be expected at the same place.

d. The CH_2 Stretching Vibrations. The calculated VSCF frequencies of molecules containing CH_2 groups are summarized in Table 7. Unlike for CH_3, the position of both symmetric and asymmetric CH_2 absorption bands is highly dependent on the neighboring groups. This trend is also supported by the experimental data. The difference of corresponding mode frequencies of ethylene (containing C═C bond) and cyclopropane (containing the simplest and unstable cycle) is about 20 cm^{-1}. The frequencies of butane CH_2 modes are even lower than those of CH_3 modes. The main reason is that this molecule is aliphatic and we could see some mixing of CH_2 and CH_3 modes, which was discussed in ref 19. The analysis of dodecane vibrational modes carried out by scaled PM3 method discussed in ref 18 showed that CH_2 frequencies are higher than CH_3 ones, which is in accordance with the data obtained for all molecules, except for butane. The reported dodecane CH_2 frequencies were between those of butane and the two molecules containing only CH_2 groups (ethylene and cyclopropane). All of these facts support the hypothesis that the CH_2 frequencies strongly depend on the surrounding groups. We can also see that the CH_2 frequencies are in almost all cases higher than the CH_3 ones. The difference between symmetric and asymmetric band frequencies is in general much bigger than the difference between CH_2 and CH_3 frequencies.

Table 7. Calculated Frequencies of C−H Vibrations in Molecules Containing CH_2 Groups

	CH_2 sym		CH_2 asym	
molecule	transitions	frequency range (cm^{-1})	transitions	frequency range (cm^{-1})
ethylene	2	3003−3043	2	3068−3097
cyclopropane	3	2982−3027	3	3046−3094
butane[a]	2	2881−2895	4	2894−2953

[a]The results for butane were already presented in ref 19.

dx.doi.org/10.1021/jp4014674 | J. Phys. Chem. A 2013, 117, 7442−7452

The spectrum of ethylene shows a puzzling discrepancy between theory and experiment. The experimental spectrum shows four distinct peaks, whereas the theoretical calculation yields two peaks. Based on the symmetry of the molecule, as shown in Table 4, the selection rules indeed suggest that only two fundamentals should carry intensity in this region. One CH_2 symmetric and one CH_2 asymmetric transition is forbidden in IR and visible in Raman, the other two transitions (again, one symmetric and one asymmetric) are forbidden in Raman and visible in IR. A possible explanation for the discrepancy is that vibrational−rotational coupling effects distort the molecule and break the selection rules. The relatively high temperature of the experiment and the small moment of inertia of ethylene seem suitable for such an explanation. Actual examination of this interpretation requires treatment of rotational effects in vibrational spectroscopy, which is not available for the VSCF method used.

4. CONCLUDING REMARKS

In this study of molecules containing CH_2 and CH_3 groups we found very good agreement between VSCF calculations and experimental measurements for all the molecules explored. The study presents detailed assignments for CH_2 and CH_3 symmetric and asymmetric stretches to the experimental IR absorption and Raman bands for these systems. The analysis of the assignments of C−H stretches shows in all cases clear separation between symmetric and asymmetric bands. The frequency difference between symmetric and asymmetric bands is in general larger than the difference between CH_2 and CH_3 frequencies. This supports the assignments of dodecane Raman bands that were based on VSCF calculations, whereas the conventional assignment is very different.[59] We found that the CH_3 bands are always located in the same place, whereas the CH_2 band location in the spectra varies. These results provide reliable tools for spectroscopic studies of organic molecules containing CH_2 and CH_3 groups, such as hydrocarbons, lipids and proteins. Comparison between BLYP, B3LYP and MP2 potentials shows that the VSCF B3LYP method exhibits the best agreement with the experimental data.

AUTHOR INFORMATION

Author Contributions

[§]Authors with equal contributions.

Notes

The authors declare no competing financial interest.

ACKNOWLEDGMENTS

Research at the Hebrew University was supported under the auspices of the Saerree K. and Louis P. Fiedler Chair in chemistry (R.B.G.). J.Š. thanks the HU for a postdoctoral Golda Meir Fellowship for the years 2011−2012. E.O.P. is grateful for financial support from the NSF Center for Chemistry at the Space-Time Limit, CHE-0802913.

REFERENCES

(1) Weissermel, K.; Arpe, H. *Industrial Organic Chemistry*: Verlag Chimie: New York, 1978.

(2) Olah, G. A.; Molnár, Á. *Hydrocarbon Chemistry*; Wiley: New York, 1995.

(3) Guo, H.; Zou, S. C.; Tsai, W. Y.; Chan, L. Y.; Blake, D. R. Emission Characteristics of Nonmethane Hydrocarbons from Private Cars and Taxis at Different Driving Speeds in Hong Kong. *Atmos. Environ.* **2011**, *45*, 2711−2721.

(4) Kolesnikov, A.; Kutcherov, V. G.; Goncharov, A. F. Methane-Derived Hydrocarbons Produced under Upper-Mantle Conditions. *Nat. Geosci.* **2009**, *2*, 566−570.

(5) Formisano, V.; Atreya, S.; Encrenaz, T.; Ignatiev, N.; Giuranna, M. Detection of Methane in the Atmosphere of Mars. *Science* **2004**, *306*, 1758−1761.

(6) Cheng, J. X.; Xie, X. S. Coherent anti-Stokes Raman Scattering Microscopy: Instrumentation, Theory and Applications. *J. Phys. Chem. B* **2004**, *108*, 827−840.

(7) Freudiger, C. W.; Min, W.; Saar, B. G.; Lu, S.; Holtom, G. R.; He, C.; Tsai, J. C.; Kang, J. X.; Xie, X. S. Label-Free Biomedical Imaging with High Sensitivity by Stimulated Raman Scattering Microscopy. *Science* **2008**, *322*, 1857−1861.

(8) Evans, C. L.; Potma, E. O.; Puoris'haag, M.; Cote, D.; Lin, C. P.; Xie, X. S. Chemical Imaging of Tissue in Vivo with Video-Rate Coherent Anti-Stokes Raman Scattering Microscopy. *Proc. Natl. Acad. Sci. U. S. A.* **2005**, *102*, 16807−16812.

(9) Lim, R. S.; Suhalim, J. L.; Miyazaki-Anzai, S.; Miyazaki, M.; Levi, M.; Potma, E. O.; Tromberg, B. J. Identification of Cholesterol Crystals in Plaques of Atherosclerotic Mice Using Hyperspectral CARS Imaging. *J. Lipid Res.* **2011**, *52*, 2177−2186.

(10) Cheng, J. X.; Volkmer, A.; Book, L. D.; Xie, X. S. Multiplex Coherent Anti-Stokes Raman Scattering Microspectroscopy and Study of Lipid Vesicles. *J. Phys. Chem. B* **2002**, *106*, 8493−8498.

(11) Lu, R.; Gan, W.; Wu, B. H.; Zhang, Z.; Guo, Y.; Wang, H. F. C-H Stretching Vibrations of Methyl, Methylene and Methine Groups at the Vapor/Alcohol (n=1−8) Interfaces. *J. Phys. Chem. B* **2005**, *109*, 14118−14129.

(12) Murphy, W. F.; Fernandezsanchez, J. M.; Raghavachari, K. Harmonic Force-Field and Raman Scattering Intensity Parameters of n-Butane. *J. Phys. Chem.* **1991**, *95*, 1124−1139.

(13) Durig, J. R.; Feng, F. S.; Wang, A. Y.; Phan, H. V. Conformational Stability, Barriers to Internal Rotation, Ab Initio Calculations, and Vibrational Assignment of 2-Butanone. *Can. J. Chem.* **1991**, *69*, 1827−1844.

(14) Durig, J. R.; Wang, A.; Beshir, W.; Little, T. S. Barrier to Asymmetric Internal-Rotation, Conformational Stability, Vibrational-Spectra and Assignments, and Ab Initio Calculations of n-Butane-d0, n-Butane-d5 and n-Butane-d10. *J. Raman Spectrosc.* **1991**, *22*, 683−704.

(15) Bowman, J. M. The Self-Consistent-Field Approach to Polyatomic Vibrations. *Acc. Chem. Res.* **1986**, *19*, 202−208.

(16) Brauer, B.; Gerber, R. B.; Kabeláč, M.; Hobza, P.; Bakker, J. M.; Riziq, A. G. A.; de Vries, M. S. Vibrational Spectroscopy of the G•••C Base Pair: Experiment, Harmonic and Anharmonic Calculations, and the Nature of the Anharmonic Couplings. *J. Phys. Chem. A* **2005**, *109*, 6974−6984.

(17) Chaban, G. M.; Jung, J. O.; Gerber, R. B. Anharmonic Vibrational Spectroscopy of Glycine: Testing of Ab initio and Empirical Potentials. *J. Phys. Chem. A* **2000**, *104*, 10035−10044.

(18) Šebek, J.; Pele, L.; Potma, E. O.; Gerber, R. B. Raman Spectra of Long Chain Hydrocarbons: Anharmonic Calculations, Experiment and Implications for Imaging of Biomembranes. *Phys. Chem. Chem. Phys.* **2011**, *13*, 12724−12733.

(19) Pele, L.; Šebek, J.; Potma, E. O.; Gerber, R. B. Raman and IR Spectra of Butane: Anharmonic Calculations and Interpretation of Room Temperature Spectra. *Chem. Phys. Lett.* **2011**, *515*, 7−12.

(20) Gregoire, G.; Gaigeot, M. P.; Marinica, D. C.; Lemaire, J.; Schermann, J. P.; Desfrancois, C. Resonant Infrared Multiphoton Dissociation Spectroscopy of Gas-Phase Protonated Peptides. Experiments and Car-Parrinello Dynamics at 300 K. *Phys. Chem. Chem. Phys.* **2007**, *9*, 3082−3097.

(21) Gaigeot, M. P.; Sprik, M. Ab initio Molecular Dynamics Computation of the Infrared Spectrum of Aqueous Uracil. *J. Phys. Chem. B* **2003**, *107*, 10344−10358.

(22) Car, R.; Parrinello, M. Unified Approach for Molecular-Dynamics and Density-Functional Theory. *Phys. Rev. Lett.* **1985**, *55*, 2471−2474.

(23) Barone, V. Anharmonic Vibrational Properties by a Fully Automated Second-Order Perturbative Approach. *J. Chem. Phys.* **2005**, *122*, 014108.
(24) Frisch, M. J.; Trucks, G. W.; Schlegel, H. B.; et al. *GAUSSIAN03*, revision C.01; Gaussian, Inc.: Pittsburgh, PA, 2003.
(25) Bowman, J. M. Self-Consistent Field Energies and Wavefunctions for Coupled Oscillators. *J. Chem. Phys.* **1978**, *68*, 608−610.
(26) Chaban, G. M.; Jung, J. O.; Gerber, R. B. Ab initio Calculation of Anharmonic Vibrational States of Polyatomic Systems: Electronic Structure Combined with Vibrational Self-Consistent Field. *J. Chem. Phys.* **1999**, *111*, 1823−1829.
(27) Gerber, R. B.; Chaban, G. M.; Brauer, B.; Miller, Y. *Theory and Applications of Computational Chemistry: The First 40 Years*; Eklsevier: Amsterdam, 2005; Chapter 9, pp 165−193
(28) Scott, A. P.; Radom, L. Harmonic Vibrational Frequencies: An Evaluation of Hartree-Fock, Moller-Plesset, Quadratic Configuration Interaction, Density Functional Theory and Semiempirical Scale Factors. *J. Phys. Chem.* **1996**, *100*, 16502−16513.
(29) Sinha, P.; Boesch, S. E.; Gu, C. M.; Wheeler, R. A.; Wilson, A. K. Harmonic Vibrational Frequencies: Scaling Factors for HF, B3LYP, and MP2 Methods in Combination with Correlation Consistent Basis Sets. *J. Phys. Chem. A* **2004**, *108*, 9213−9217.
(30) Schmidt, M. W.; Baldridge, K. K.; Boatz, J. A.; Elbert, S. T.; Gordon, M. S.; Jensen, J. H.; Koseki, S.; Matsunaga, N.; Nguyen, K. A.; Su, S. J.; Windus, T. L.; Dupuis, M.; Montgomery, J. A. General Atomic and Molecular Electronic-Structure System. *J. Comput. Chem.* **1993**, *14*, 1347−1363.
(31) Pele, L.; Gerber, R. B. On the Number of Significant Mode-Mode Anharmonic Couplings in Vibrational Calculations: Correlation-Corrected Vibrational Self-Consistent Field Treatment of Di-, Tri-, and Tetrapeptides. *J. Chem. Phys.* **2008**, *128*, 165105.
(32) Brauer, B.; Pincu, M.; Buch, V.; Bar, I.; Simons, J. P.; Gerber, R. B. Vibrational Spectra of alpha-Glucose, beta-Glucose, and Sucrose: Anharmonic Calculations and Experiment. *J. Phys. Chem. A* **2011**, *115*, 5859−5872.
(33) Becke, A. D. Density-Functional Exchange-Energy Approximation with Correct Asymptotic Behavior. *Phys. Rev. A* **1988**, *38*, 3098−3100.
(34) Becke, A. D. Density-Functional Thermochemistry 0.3. The Role of Exact Exchange. *J. Chem. Phys.* **1993**, *98*, 5648−5652.
(35) Møller, C.; Plesset, M. S. Note on an Approximation Treatment for Many-Electron Systems. *Phys. Rev. Lett.* **1934**, *46*, 618−622.
(36) Dunning, T. H., Jr. Gaussian Basis Sets for Use in Correlated Molecular Calculations. I. The Atoms Boron through Neon and Hydrogen. *J. Chem. Phys.* **1989**, *90*, 1007−1023.
(37) Kendall, R. A.; Dunning, T. H., Jr.; Harrison, R. J. Electron-Affinities of the 1st-Row Atoms Revisited - Systematic Basis -Sets and Wave-Functions. *J. Chem. Phys.* **1992**, *96*, 6796−6806.
(38) Chaban, G. M.; Gerber, R. B. Anharmonic Vibrational Spectroscopy Calculations with Electronic Structure Potentials: Comparison of MP2 and DFT for Organic Molecules. *Theor. Chem. Acc.* **2008**, *120*, 273−279.
(39) Gerber, R. B.; Ratner, M. A. Semi-Classical Self-Consistent Field (Sc Scf) Approximation for Eigenvalues of Coupled-Vibration Systems. *Chem. Phys. Lett.* **1979**, *68*, 195−198.
(40) Gerber, R. B.; Ratner, M. A. Self-Consistent-Field Methods for Vibrational Excitations in Polyatomic Systems. *Adv. Chem. Phys.* **1988**, *70*, 97−132.
(41) Gregurick, S. K.; Fredj, E.; Elber, R.; Gerber, R. B. Vibrational Spectroscopy of Peptides and Peptide-Water Complexes: Anharmonic Coupled-Mode Calculations. *J. Phys. Chem. B* **1997**, *101*, 8595−8606.
(42) Gregurick, S. K.; Liu, J. H.-Y.; Brant, D. A.; Gerber, R. B. Anharmonic Vibrational Self-Consistent Field Calculations as an Approach to Improving Force Fields for Monosaccharides. *J. Phys. Chem. B* **1999**, *103*, 3476−3488.
(43) Bihary, Z.; Gerber, R. B.; Apkarian, V. A. Vibrational Self-Consistent Field Approach to Anharmonic Spectroscopy of Molecules in Solids: Application to Iodine in Argon Matrix. *J. Chem. Phys.* **2001**, *115*, 2695−2701.
(44) Gerber, R. B.; Brauer, B.; Gregurick, S. K.; Chaban, G. M. Calculation of Anharmonic Vibrational Spectroscopy of Small Biological Molecules. *PhysChemComm* **2002**, *5*, 142−150.
(45) Neugebauer, J.; Hess, B. A. Fundamental Vibrational Frequencies of Small Polyatomic Molecules from Density-Functional Calculations and Vibrational Perturbation Theory. *J. Chem. Phys.* **2003**, *118*, 7215−7225.
(46) Espinoza, C.; Szczepanski, J.; Vala, M.; Polfer, N. C. Glycine and Its Hydrated Complexes: A Matrix Isolation Infrared Study. *J. Phys. Chem. A* **2010**, *114*, 5919−5927.
(47) Chaban, G. M.; Jung, J. O.; Gerber, R. B. Anharmonic Vibrational Spectroscopy of Hydrogen-Bonded Systems Directly Computed from ab initio Potential Surfaces: (H2O)(n), n=2, 3; Cl-(H2O)(n), n=1, 2; H+(H2O)(n), n=1, 2; H2O-CH3OH. *J. Phys. Chem. A* **2000**, *104*, 2772−2779.
(48) Christiansen, O.; Luis, J. M. Beyond Vibrational Self-Consistent-Field Methods: Benchmark Calculations for the Fundamental Vibrations of Ethylene. *Int. J. Quantum Chem.* **2005**, *104*, 667−680.
(49) Christiansen, O. Vibrational Structure Theory: New Vibrational Wave Function Methods for Calculation of Anharmonic Vibrational Energies and Vibrational Contributions to Molecular Properties. *Phys. Chem. Chem. Phys.* **2007**, *9*, 2942−2953.
(50) Seidler, P.; Kaga, T.; Yagi, K.; Christiansen, O.; Hirao, K. On the Coupling Strength in Potential Energy Surfaces for Vibrational Calculations. *Chem. Phys. Lett.* **2009**, *483*, 138−142.
(51) Roy, T. K.; Gerber, R. B. Vibrational Self-Consistent Field Calculations for Spectroscopy of Biological Molecules: New Algorithmic Developments and Applications. *Phys. Chem. Chem. Phys.* **2013**, *15*, 9468−9492.
(52) Carter, S.; Culik, S. J.; Bowman, J. M. Vibrational Self-Consistent Field Method for Many-Mode Systems: A New Approach and Application to the Vibrations of CO Adsorbed on Cu(100). *J. Chem. Phys.* **1997**, *107*, 10458−10469.
(53) Jung, J. O.; Gerber, R. B. Vibrational Wave Functions and Spectroscopy of (H2O)(n), n=2, 3, 4, 5: Vibrational Self-Consistent Field with Correlation Corrections. *J. Chem. Phys.* **1996**, *105*, 10332−10348.
(54) Norris, L. S.; Ratner, M. A.; Roitberg, A. E.; Gerber, R. B. Møller-Plesset Perturbation Theory Applied to Vibrational Problems. *J. Chem. Phys.* **1996**, *105*, 11261−11267.
(55) Pele, L.; Brauer, B.; Gerber, R. B. Acceleration of Correlation-Corrected Vibrational Self-Consistent Field Calculation Times for Large Polyatomic Molecules. *Theor. Chem. Acc.* **2007**, *117*, 69−72.
(56) Benoit, D. M. Efficient Correlation-Corrected Vibrational Self-Consistent Field Computation of OH-Stretch Frequencies Using a Low-Scaling Algorithm. *J. Chem. Phys.* **2006**, *125*, 244110−244111.
(57) Christiansen, O. Moller-Plesset Perturbation Theory for Vibrational Wave Functions. *J. Chem. Phys.* **2003**, *119*, 5773−5781.
(58) Knaanie, R.; Šebek, J.; Kalinowski, J.; Gerber, R. B. Hybrid MP2/MP4 Potential Surfaces in VSCF Calculations of IR Spectra: Applications for Organic Molecules. *Spectrochim. Acta, Part A* **2013**, DOI: http://dx.doi.org/10.1016/j.saa.2013.06.035.
(59) Spiker, R. C.; Levin, I. W. Raman Spectra and Vibrational Assignments for Dipalmitoyl Phosphatidylcholine and Structurally Related Molecules. *Biochim. Biophys. Acta* **1975**, *388*, 361−373.